MICROTENSION TEST METHOD FOR MEASURING TENSILE PROPERTIES OF INDIVIDUAL CELLULOSIC FIBERS

Ge Wang†
Staff Scientist

Yan Yu
Associate Scientist
International Center for Bamboo and Rattan
Beijing, China

*Sheldon Q. Shi**†
Assistant Professor

Jinwu Wang
Post-Doctoral Research Associate
Forest Products Department
Mississippi State University
Mississippi State, MS 39759

Shuangping Cao
Graduate Research Assistant

Haitao Cheng
Research Associate
International Center for Bamboo and Rattan
Beijing, China

(Received October 2010)

Abstract. A microtension testing system was devised to measure mechanical properties of individual cellulosic fibers. To avoid specimen gripping and to enhance fiber alignment during testing, a self-aligning ball and socket gripping assembly was used in the microtensile tester design. A resolution of 0.098 mN was obtained for the tensile load measurement with this microtensile tester. Fiber strain was determined from high-precision stepper motor movement with 0.078-μm resolution or by in situ video photography. Cross-sectional areas of a single fiber cell wall were measured with a confocal laser scanning microscope. Results obtained from this system indicated a linear stress–strain curve until fatal failure for mature latewood fibers, whereas juvenile latewood fibers displayed curvilinear stress–strain relationships. Average values of tensile strength, tensile modulus, and elongation at break were 1258 MPa, 19.9 GPa, and 6.6% for mature latewood fiber and 558 MPa, 8.5 GPa, and 9.9% for juvenile latewood fiber, respectively. These values agreed with published data. The preliminary test indicated the usefulness of the integrated environmental chamber for investigating moisture effect on fiber engineering properties, but further investigation is needed to obtain statistically significant data.

Keywords: Tensile properties, microtension, cellulosic fibers, microtester, Chinese fir.

INTRODUCTION

Cellulosic fibers from wood, bamboo, kenaf, and other plants are typically used for pulp and paper, textiles, and cordage. However, recently,

* Corresponding author: sshi@cfr.msstate.edu
† SWST member

expanding their use in automotive components, soundproofing and thermal insulation, and composites has been intensively investigated to conserve natural resources and decrease dependence on petroleum-based products (John and Thomas 2008). Properties required for good fiber reinforcement in a polymeric matrix include great strength and modulus, good dispersion, less hygroscopicity, and good compatibility between fiber and matrix. Tailoring natural fibers for high-performance biocomposites demands fundamental understanding of natural fiber characteristics. Characterizing cellulosic fibers is important for current research in this area. Quantitatively characterizing micromechanical properties of individual natural fibers will help select the most appropriate fiber species and decordication processes for the targeted composite grade. Investigating micromechanical properties of individual fibers is essential to elucidate the relationships among plant structure, especially cell wall structure, cell wall properties, and functionality of resulting products.

However, very few analytical instruments are available for accurately measuring mechanical properties of individual cellulosic fibers in micron size. Cellulosic fibers from kenaf, bamboo, softwood, and other bast fibers are typically 1-5 mm long and have a 10-50 μm diameter. Each fiber consists of a cell wall that surrounds an inner cavity called lumen. Such individual fibers, small in diameter and tubular and tapered in shape, present challenges in preparation, mounting, gripping, and testing of mechanical properties in a conventional universal test machine.

Because individual fiber characterization is inconvenient, the final product is usually used to evaluate performance and quality of a fiber, which can be costly and time-consuming. For example, in pulping, a sheet of fibers is formed for evaluating fiber strength. For bast fibers, about 10-40 elementary individual fibers are assembled together into a bundle bonded by pectin, which is comparable in size and shape to a long continuous filament of synthetic or regenerated single fibers. Single fiber test standards such as ASTM D3822 for Tensile Properties of Single Textile Fibers and C 1557 for Tensile Strength and Young's Modulus of Fibers have been widely followed to provide acceptable strength and modulus measurements of bast and bamboo fiber bundles (Rao and Rao 2007; Xue et al 2009; Ochi 2010). The tension test on a fiber bundle has some advantages; it is faster, easier, and more practical. However, in fiber reinforcement applications such as fiber-reinforced polymer composites, cellulosic fibers are usually pulped into individual cells to facilitate uniform dispersion in matrix and large surface adhesion area. Therefore, properties of individual fibers are of interest for composite modeling and simulation to provide an accurate predictive design. To obtain microtensile properties of individual fibers, a specially designed microtension tester was developed that is able to characterize individual fibers on a micro scale.

Consequently, customized techniques and procedures have been investigated for stressing individual fibers. The atomic force microscope (AFM) has been shown to be a useful tool to measure lateral flexibility of individual fibers (Navaranjan et al 2008). However, maximum load and sample elongation are limited for the AFM, and sample preparation and handling still remain a challenge (Tan and Lim 2006). In terms of cell wall mechanics, nanoindentation allows for local hardness and stiffness to be directly measured at a submicron level (Xing et al 2009; Adusumalli et al 2010). However, the orthotropic nature of a cell wall prevents direct measurement of the longitudinal elastic modulus of wood cell walls by nanoindentation (Gindl and Schoberl 2004). Various micromechanical devices have been developed to test silicon and many other thin films for microelectromechanical systems. The issue of specimen gripping and alignment could be resolved by cofabricating the specimen with the actuator during the microelectronic fabrication process (Kamat 2009). However, the microfabrication process cannot be easily adapted for biological or polymeric samples (Tan and Lim 2004).

Uniaxial tensile forces on whole individual fibers are generally used in the composite property prediction because such fiber forms are commonly

used as raw materials for the composites. The main elements of such a microtensile device include a method to apply force to a fiber and precise measurement of applied force and resultant fiber elongation. Techniques are necessary for mounting the fiber in a tensile apparatus without inducing stress concentration on the fiber. Jayne (1960) tensioned individual fibers in a universal testing machine with abrasive paper for clamping. Burgert et al (2003) favored a frame construction as a fiber carrier mounted on a microtensile apparatus. A ball and socket type grip assembly attached to an in-house miniature material tester has been widely accepted as the most appropriate for testing individual cellulosic fibers (Mott et al 1995; Groom et al 2002; Tchepel et al 2006).

Load cells sensitive enough to detect small forces are available in current technology, however, precise measurement of fiber elongation is much more difficult to achieve. In most instances, fiber strain is calculated according to crosshead movement as a function of time (Groom et al 2002). Compared with pure fiber behavior, elasticity of the tensile apparatus and displacements in the gripping assembly apparently resulted in greater elongation (Kompella and Lambros 2002). Strain of fiber under tension can also be measured by tracking the difference of two line marks on digital photography images (Burgert et al 2003). However, a light microscope at this magnification does not provide sufficient resolution for performing image analysis for strain detection on fibers. Fixing artificial reference markers on the fiber itself is difficult and might damage the specimen (Burgert et al 2003).

The overall objective of this research was to develop an experimental technique that can be commonly used to characterize individual cellulosic fibers for targeted applications. This article reports microtensile test system development. Individual fibers from latewood of Chinese fir were used. Tensile modulus and strength of individual fibers from Chinese fir latewood were measured and compared with those in the literature. In subsequent separate articles, the technique will be used to evaluate differences in stiffness and strength of individual fibers from different species and agricultural stems.

MATERIALS AND METHODS

Sample Preparations

Blocks of 30-yr-old Chinese fir latewood ($30 \times 10 \times 1$ mm^3) were cut in the longitudinal tangential direction from the 5th and 26th growth rings. Chinese fir was harvested from a tree farm in China, and samples were taken from a tree height of 1.5 m. The blocks were processed into small, thin sticks. These sticks were immersed in a solution of hydrogen peroxide and glacial acetic acid (at a molar ratio of 1:1) and then placed in an oven at 60°C for about 24 h. The samples were taken out and washed thoroughly first with tap water and then with deionized water five times. Individual fibers (tracheids) were separated mechanically using fine tweezers and then stored at a target temperature of 25°C and 40% RH.

Microtensile Test System

A microtensile test system was developed to provide 1) easiness of handling individual fibers; 2) precision of force and displacement measurement; and 3) precision of cross-sectional area measurement of individual fibers. The developed tensile test system (called SF-1 microtester) consists of two ball and socket type grips inside an environmental chamber, a force sensor (UL-10GR; Minebea Co. Ltd., Tokyo, Japan), a three-dimensional adjustable stage with an attached high-precision linear ball bearing slide (SKF, Gothenburg, Sweden), two horizontal and vertical CCD cameras with macro lenses (Daheng, Beijing, China; DH-HV1303UM, 1280×1024), and a stepper motor (Oriental Motor, Torrance, CA). Figure 1 shows the tensile test system, and Fig 2 shows the control diagram. The three-dimensional adjustable stage is bolted tightly to the base of the instrument. The force sensor and stepper motor attached to the adjustable table are in such good alignment that rotation of the

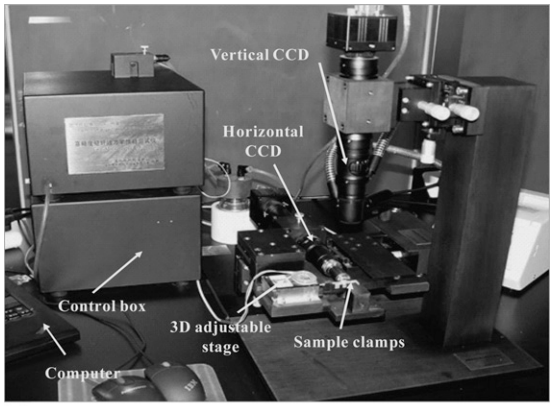

(a)

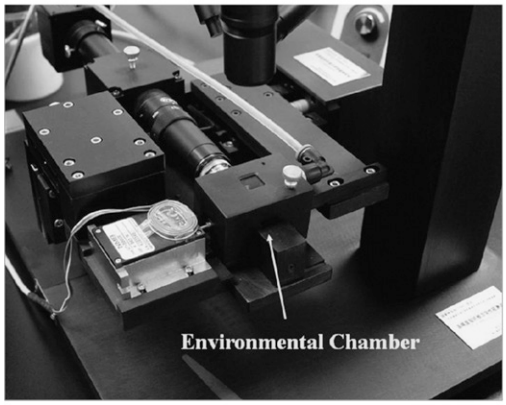

(b)

Figure 1. Microtension test system (SF-1 Microtester I); (a) environmental chamber off; (b) environmental chamber on.

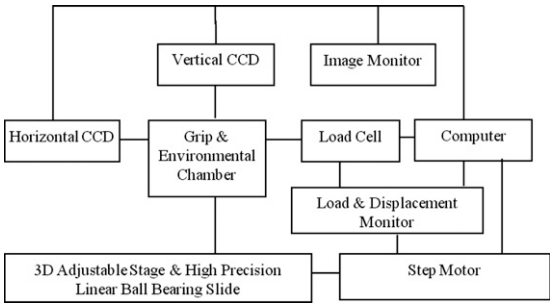

Figure 2. Diagram of microtester components.

stepper motor can apply a force to fiber through the force sensor. The system was designed to measure tensile modulus, strength, creep, relaxation, and cyclic loading characteristics as well as moisture effect on tensile properties of a fiber in micron scale.

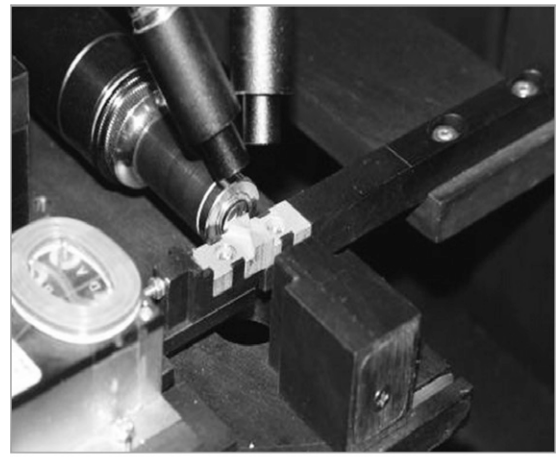

(a)

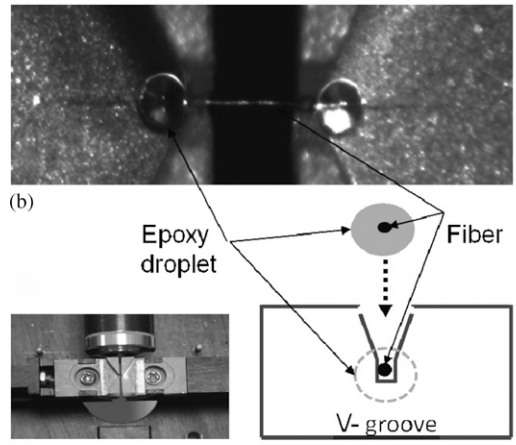

(b) (c) (d)

Figure 3. (a) and (c) Gripping assembly without environmental chamber showing horizontal and vertical cameras and lighting tube in (a); (b) individual fiber under 10-mN pretension and nominal 0.7-mm gauge length between two opposing droplets held by V-grooves; (d) positioning sample into the V-groove.

Fiber attachment onto the grips was critical to obtain an accurate measurement. Figures 3a and c show the fiber gripping assembly. Figure 3d shows a sample being positioned into a V-groove. The sample was prepared in a way that two epoxy resin droplets were formed near two ends of an individual fiber (Fig 4). These resin balls were then positioned into the V-grooves of the grips to form a ball and socket type assembly. The fiber was then bonded rigidly on grips with adhesive. This gripping has been proven to

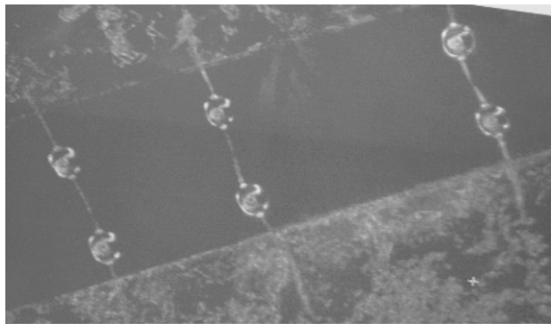

Figure 4. Prepared specimens with two adhesive droplets near ends of fiber.

minimize the problems of fiber misalignment and fiber crushing failure near the clamps (Mott et al 1995; Groom et al 2002; Tchepel et al 2006). It also allows rapid replacement of fibers once they have ruptured, thus ensuring a substantial number of fibers can be tested within a short period. The three-dimensional adjustable stage connected with one of two grips can further align the fiber lengthwise with applied force direction, which further decreased fiber misalignment, stress concentration, and associated premature cell wall failure.

The environmental chamber assembly is shown in Fig 1b. RH and temperature can be controlled in the range of 40-95% at room temperature, which enables investigation of moisture effects on fiber tensile properties.

Two high-resolution CCD with macro zoom lenses (3.5×-25×) were used to obtain in situ images of the individual fiber during tension testing for the purposes of assisting the fiber into the ball and socket griping assembly and to adjust fiber alignment in the force direction. Video images were used for measuring initial gauge length and fiber strain.

Loading is actuated by the stepper motor with an attached high-precision linear ball bearing slide connecting to one end of the fiber through one grip. The opposite end of the fiber is connected with a load cell through the other grip. Both ends are attached by resin droplets. Two NMB force sensors (Minebea Co., Ltd., Tokyo, Japan) are used. The rated capacity of one sensor is 4.903 N with 0.49-mN resolution; the other is 980.7 mN with 0.098-mN resolution. The motion of the stepper motor is controlled by computer, and the position is registered in real time by a data acquisition unit. The stepper motor has a gradation of 0.1125° of each step, enabling a linear motion of slide with a resolution of 0.078 μm. Traveling distance of the slide is 12.5 mm. In this configuration, displacement can be determined by the stepper motor movement as a function of time. Compared with pure fiber behavior however, the obtained displacement arising from stepper motor movement includes a component caused by tensile apparatus compliance, which has been adjusted by calibration practice. This displacement component has also been minimized through instrumental design using the stiff parts between the fiber and stepper motor.

Accurate tensile testing requires direct strain measurement in the gauge section. To measure only the strain of the individual fiber directly, fiber length between epoxy resin beads can be tracked by acquiring images of the fiber during the tension process. Strain can be calculated from the difference of the end points of beads on the images. Because load, displacement, and images are all recorded on a common time base, it is possible to correlate specific images to corresponding load displacement information.

Tensile Test Method

Tensile properties of individual fibers were tested using a 980.7-mN load cell with a resolution of 0.098 mN. Under the assistance of a stereomicroscope, fibers were placed across a slot of 1.8 mm in a Plexiglas plate and two ends of the fiber were taped to the rims of the slot. Two epoxy droplets about 50 μm in diameter were placed near the ends of the fiber with fine tweezers (Fig 4). The epoxy used in this study was a high-strength, two-part, 30-min slow-cure adhesive obtained from Hare's Hobby Shop LLC (Alexandria, LA). Epoxy to hardener ratio was 56:44. The Plexiglas plates carrying individual fibers were dried at 60°C

for 24 h and cooled at 25°C and 40% RH overnight. The epoxy resin was not observed to penetrate or flow along the fiber cell wall after curing. The fiber with two cured epoxy droplets was then taken off the Plexiglas plate and positioned into the ball and socket grips monitored with vertical and horizontal CCD cameras. Fiber length and force direction were aligned with the three-dimensional adjustable stage. A 10-mN force was applied to straighten the fiber by prestressing. An image of fiber under prestressing was taken with the vertical CCD camera. By image analysis, the distance between the two droplets on the fiber was measured as the gauge length for fiber strain measurement. Displacement channels were first zeroed. Tests were displacement-controlled using a constant strain rate of 0.8 μm/s. The fiber was removed from the grips immediately on failure and stored for subsequent cross-sectional area measurement with a confocal laser scanning microscope (CLSM). Thirty fibers were tested for each fiber type at 25°C and 40% RH. A preliminary test at 25°C and 90% RH was conducted to evaluate usefulness of the environmental chamber. The fiber was positioned onto grips inside the environmental chamber without pretension and was exposed in this environment for 1 h to equilibrate with new conditions (storage conditions were 25°C and 40% RH) before they were actually tensioned.

Cross-Sectional Area of the Cell Wall

Because of the lumen in the fiber, the cross-sectional area of the annular cell wall is substantially smaller than the overall fiber cross-sectional area (Eder et al 2009). For different cellulosic fiber types, lumen size can be different. Fiber tensile stress and stiffness values depend on which cross-sectional areas are used: overall fiber or cell wall area only. In the literature, fiber cross-sectional areas were calculated from the fiber outer diameter, usually recorded in micrometers for fiber bundles or using an optical microscope (Rao and Rao 2007; Symington et al 2009). However, fiber cross-sectional areas calculated by the diameter involve some degrees of error because fiber cross-sections are not necessary circular (Munawar et al 2007). Also, fiber shape and cross-sectional area are not constant lengthwise.

In this study, CLSM (LSM 510 Meta; Zeiss, Oberkochen, Germany) was used to obtain the cross-section image. CLSM has better lateral resolution than conventional optical microscopes, and specimen preparation is simplified compared with that for electron microscopy (Jang et al 1992). Epoxy droplets of tested fibers were removed under a stereomicroscope with microscissors. To enable fibers to fluoresce when subjected to laser excitation, they were stained in a 0.001% (w/v) acridine orange solution for 4 min at room temperature. Fibers were then attached to glass slides with the aid of tissue tack and were ready for imaging.

An excitation wavelength of 514 nm VIS laser module from an argon laser was used. The pinhole size was set at an optimum value by Zeiss LSM control software. Emission light collected by a detector was set at a wavelength between 525 and 760 nm. Gain and offset were adjusted automatically for each fiber by the software to ensure constant image quality. Cross-sectional images were constructed from a series of vertical line scans adjacent to failure location with a scanning step size of 0.12 μm. Approximately 40 images were averaged per scan to increase the signal-to-noise ratio. Cell wall cross-sectional areas (subtracting lumen from the whole cross-sectional area) were measured by Image J analysis software (Fig 5). Cell wall cross-sectional areas were then used to convert load-elongation curves into stress–strain curves.

Microfibril Angle Measurement

An X-ray diffractometer (X'pert pro; Panalytical, Almelo, The Netherlands) was used to determine average microfibril angle (MFA) of the five samples before maceration. A point-focused X-ray beam was applied to the tangential section

with a scanning angle range of 0-360° and a scanning step of 0.5°. From obtained intensity curves of X-ray diffraction, sample MFA was determined.

RESULTS AND DISCUSSION

Physical and mechanical properties of two Chinese fir latewood fibers (mature and juvenile) are summarized in Table 1, and property distributions are shown in Fig 6. Table 1 and Fig 6 show that tensile strength and modulus values of mature fibers were more than double those of juvenile fibers. Fiber from Chinese fir mature latewood displayed a linear stress–strain relationship, whereas juvenile latewood fibers displayed a curvilinear curve (Fig 7). The average MFA was 15° for mature latewood fiber and 35° for juvenile latewood fiber (Table 1). As shown in Fig 8, MFAs of cellulosic fibers affected shapes of stress–strain curves when the fiber was under tension (Page and El-Hosseiny 1983). It can be seen that stress–strain curves of both juvenile and mature latewood fibers shown in Fig 7 are in agreement with those having similar MFAs shown in Fig 8. Mature latewood fibers with low MFAs stressed uniaxially in tension exhibited purely linear stress–strain curves. The curvilinearity of stress–strain curves of juvenile latewood fibers might have been caused by reorientation of the fibrils to the fiber axis under straining (Kolln et al 2005). The higher MFAs might also account for a higher elongation at break for juvenile fibers. In addition, concentrated pits and a thin cell wall in juvenile latewood fiber should be responsible for the lower tensile strengths of juvenile fibers (Fig 5c).

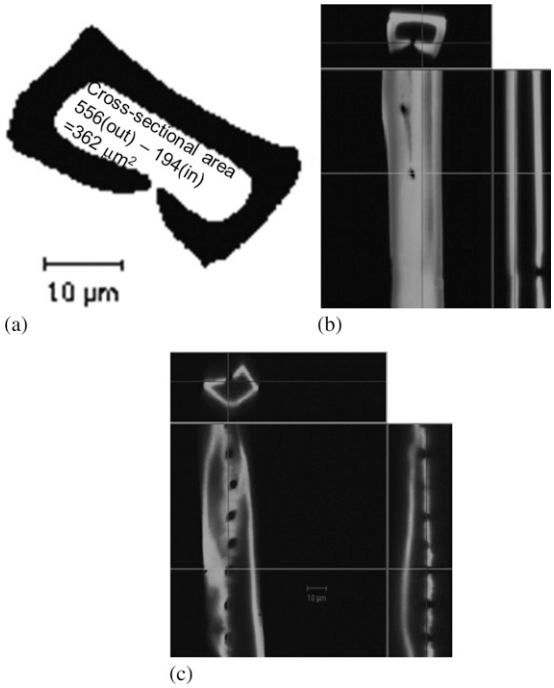

Figure 5. (a) Example of cross-sectional area measurement with analysis of image obtained by confocal laser scanning microscope, (b) mature latewood fibers, and (c) juvenile latewood fibers.

Test results obtained from the developed . microtester are well in agreement with published literature values. Groom et al (2002) used the same chemical isolation and fiber treatment. Table 2 compares characteristics of loblolly pine latewood fibers (Groom et al 2002) and Chinese fir, which was used in this study. It clearly shows that tensile modulus and tensile strength were a function of MFA and were independent from wood species (Fig 9). Measured data for the two species from the two studies agreed quite well. This is quite reasonable because the developed microtester used a similar gripping mechanism. It measured displacement in a similar way by tracking the number of turns

Table 1. Means (standard deviations) of Chinese fir latewood fibers (n = 30).

Index	Tensile strength (MPa)	Tensile modulus (GPa)	Elongation at break (%)	Maximum load (mN)	Cross area (μm^2)	Gauge length (mm)	MFA (°)
Mature	1258	19.9	6.6	284	231	0.79	15
fiber	(287)	(4.5)	(1.2)	(60)	(49)	(0.14)	(2.8)
Juvenile	558	8.5	9.9	111	203	0.54	35
fiber	(142)	(2.1)	(2.3)	(33)	(53)	(0.08)	(2.8)

MFA, microfibril angle.

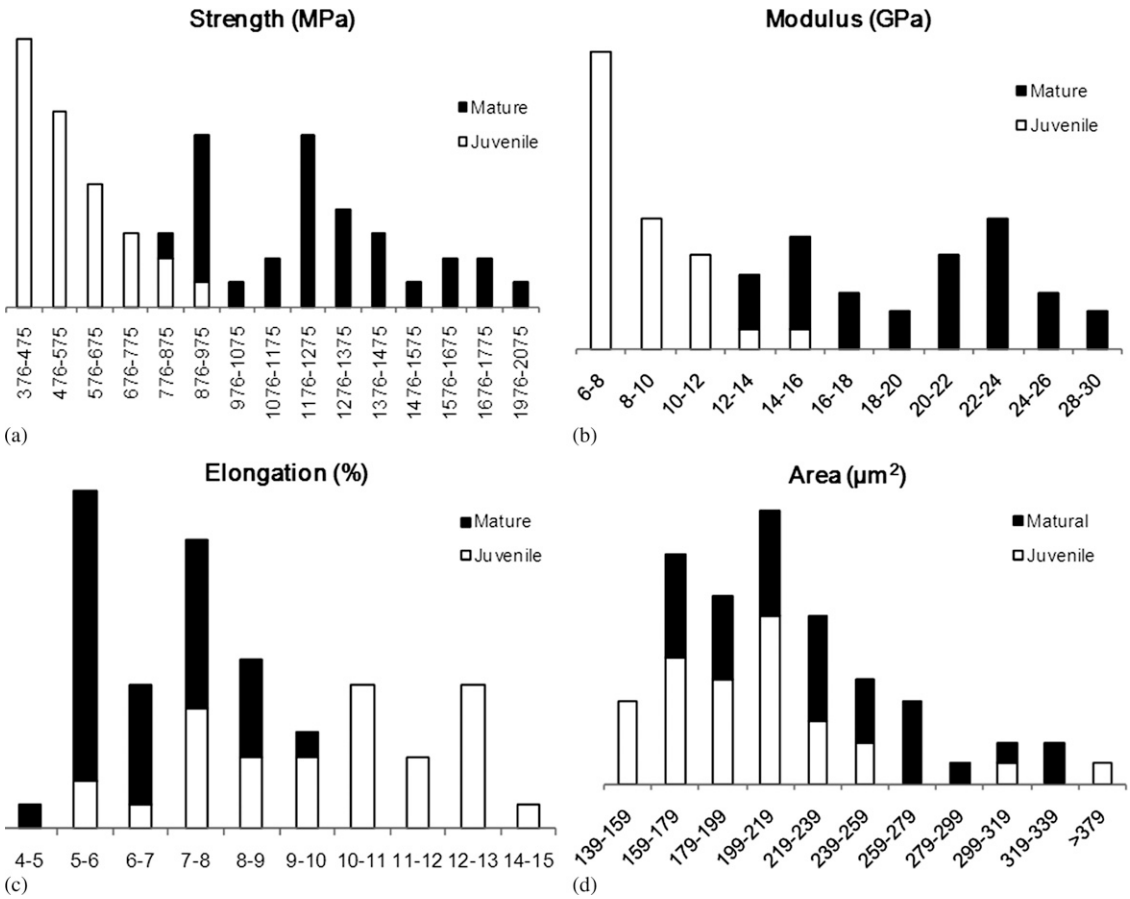

Figure 6. Property distributions of fibers from Chinese fir mature and juvenile latewood.

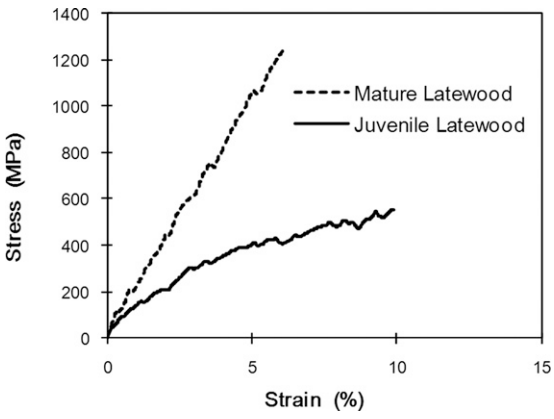

Figure 7. Typical stress–strain of Chinese fir latewood fibers.

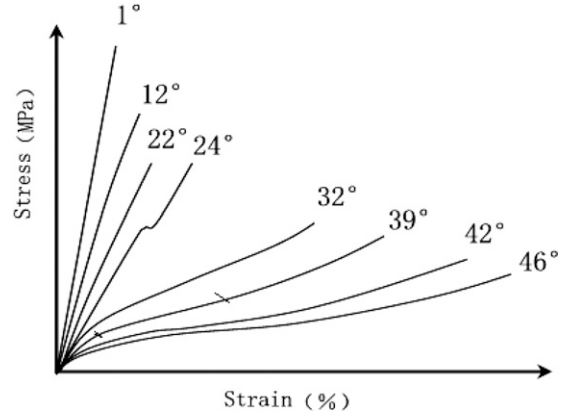

Figure 8. Effect of microfibril angles on stress–strain curves (Page and El-Hosseiny 1983).

Table 2. Characteristics of Chinese fir and loblolly pine latewood fibers.

	Ring number	MFA (deg)	Tensile modulus (GPa)	Tensile strength (MPa)	Cross-sectional area (μm^2)
Loblolly pine[a]	5	37.0	6.6	410	191
Chinese fir	5	34.9	8.5	558	203
Loblolly pine[a]	5	30.1	12.1	641	303
Chinese fir	25	15.2	19.9	1258	231
Loblolly pine[a]	10	14.6	23.5	1083	394

[a] From Groom et al (2002).
MFA, microfibril angle.

of the screw that drives the crosshead. These research results corroborated performance and repeatability of the ball and socket gripping mechanism. Also, the developed microtester is equipped with a high-resolution camera system to record the stressing of each individual fiber. Further research is underway to investigate if the digital image correlation technique can be used to measure axial displacement in a more accurate way than tracking mechanical movement. The main advantage of the proposed system is that it is a noncontact technique that does not accumulate the compliances of a mechanical measuring system (Lu et al 2003).

Eder et al (2009) obtained tensile strength and modulus of 760 MPa and 22 GPa, respectively, for mechanically separated spruce latewood fibers with average MFA of 8°. Tensile modulus values in Eder et al (2009) also fit well to data in this study, whereas this study obtained a higher tensile strength for the fibers. Tensile strength and tensile modulus measured on spruce fibers obtained from the transition zone are 1.2 and 22.6 GPa, respectively (Burgert et al 2003); they are in agreement with data in this study. Many other published values have also been compared, but large variability exists. This may be caused by variability of cellulosic natural fiber, fiber preparations for testing, and/or testing method. Many published values are lower than those in this study mainly because overall fiber cross-sectional areas were used instead of cross-sectional areas of the cell wall only (Symington et al 2009).

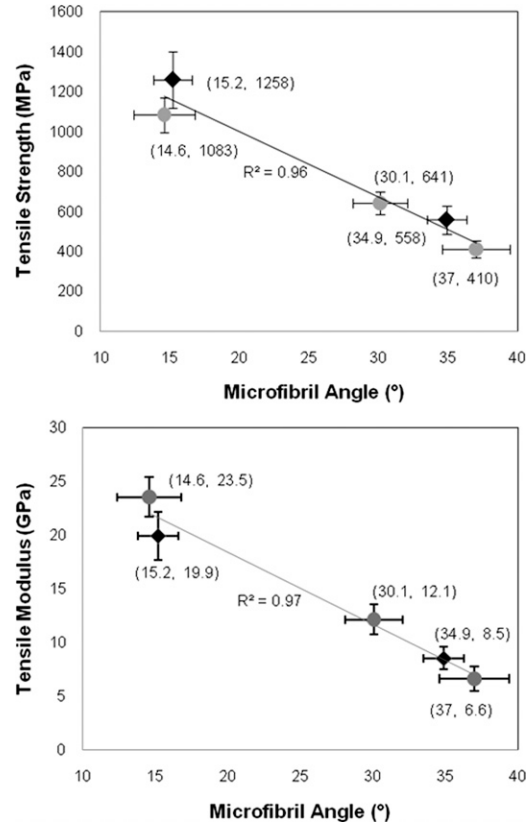

Figure 9. Tensile strength and modulus vs microfibril angle; diamonds are Chinese fir, circles are loblolly pine from Groom et al (2002); numbers in parentheses are coordinates of points. Lengths of error bars are 1 standard deviation.

MOISTURE EFFECT ON TENSILE PROPERTIES

Stress–strain curves of mature latewood fibers were obtained (Fig 10) after 1-h exposure in a small environmental chamber of 25°C and 40 and 90% RH, respectively. Curves were fitted with a linear regression equation ($y = Ax + b$). Figure 10 shows the slope (A), which is related to the modulus, of the fiber in 40% RH was greater than that in 90% RH. Apparently, the higher moisture condition plasticized the fiber. However, a 6.3% change of the slopes of 187

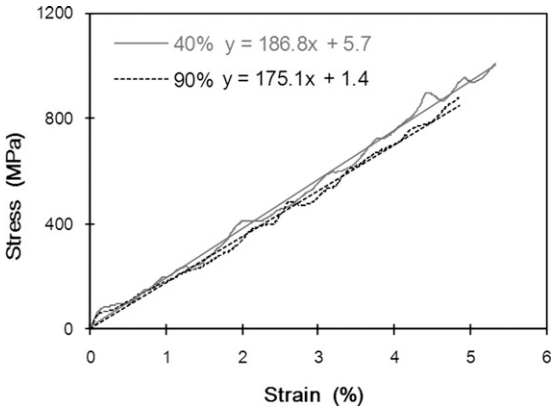

Figure 10. Stress–strain curves of Chinese fir mature latewood fibers under two humidity levels.

(40% RH) vs 175 (90% RH) is insignificant compared with the 23% coefficient of variation presented in Table 1 for the same source of specimens: mature latewood fibers (40% RH). Although this preliminary test showed the potential of the developed microtester for investigating the moisture effect on mechanical properties of individual fibers, further investigation is needed to confirm its utility with statistically significant data.

CONCLUSIONS

1. A uniaxial microtensile system, called the SF-I Microtester, to stress microscale individual cellulosic fibers in tension is presented in this article. Integration of ball and socket grips, two directional macro CCD cameras, and an adjustable x-y-z stage provided great convenience in preparation, mounting, and testing of individual cellulosic fibers in micron scale.
2. Average tensile strength and modulus for mature Chinese fir latewood fibers were more than doubled compared with that for juvenile fibers, which may have been mainly caused by MFA (15° for mature fiber and 35° for juvenile fiber).
3. The incorporated environmental chamber in the microtensile tester enabled investigation of moisture effect on tensile properties. Increased humidity levels appeared to decrease individual wood fiber stiffness values. Further research efforts will focus on evaluating moisture effect on stress–strain relationships of individual cellulosic fibers with statistically significant data.

ACKNOWLEDGMENTS

The authors would like to thank Dr. Leslie Groom and Dr. Chuang Hsu, USDA Forest Service, Alexandra Forestry Center, their suggestions in this research.

REFERENCES

Adusumalli RB, Mook WM, Passas R, Schwaller P, Michler J (2010) Nanoindentation of single pulp fibre cell walls. J Mater Sci 45(10):2558-2563.

Burgert I, Fruhmann K, Keckes J, Fratzl P, Stanzl-Tschegg SE (2003) Microtensile testing of wood fibers combined with video extensometry for efficient strain detection. Holzforschung 57(6):661-664.

Eder M, Jungnikl K, Burgert I (2009) A close-up view of wood structure and properties across a growth ring of Norway spruce (*Picea abies* [L] Karst.). Trees-Struct Funct 23(1):79-84.

Gindl W, Schoberl T (2004) The significance of the elastic modulus of wood cell walls obtained from nanoindentation measurements. Compos Part A-Appl S 35(11):1345-1349.

Groom L, Mott L, Shaler S (2002) Mechanical properties of individual southern pine fibers. Part I. Determination and variability of stress–strain curves with respect to tree height and juvenility. Wood Fiber Sci 34(1):14-27.

Jang HF, Robertson AG, Seth RS (1992) Transverse dimensions of wood pulp fibers by confocal laser scanning microscopy and image analysis. J Mater Sci 27(23): 6391-6400.

Jayne BA (1960) Wood fibers in tension. Forest Prod J 10(6):316-322.

John MJ, Thomas S (2008) Biofibres and biocomposites. Carbohydr Polym 71(3):343-364.

Kamat SV (2009) Experimental techniques for the measurement of mechanical properties of materials used in microelectromechanical systems. Def Sci J 59(6):605-615.

Kolln K, Grotkopp I, Burghammer M, Roth SV, Funari SS, Dommach M, Muller M (2005) Mechanical properties of cellulose fibres and wood. Orientational aspects in situ investigated with synchrotron radiation. J Synchrotron Radiat 12:739-744.

Kompella MK, Lambros J (2002) Micromechanical characterization of cellulose fibers. Polym Test 21(5):523-530.

Lu Z, Zarrabi K, Humphries S, Croker A, Small R (2003) Non-contacting creep strain determination at 550°C. Int J Press Vessels Piping 80(6):361-365.

Mott L, Shaler SM, Groom LH, Liang BH (1995) The tensile testing of individual wood fibers using environmental scanning electron microscopy and video image analysis. Tappi J 78(5):143-148.

Munawar SS, Umemura K, Kawai S (2007) Characterization of the morphological, physical, and mechanical properties of seven nonwood plant fiber bundles. J Wood Sci 53(2):108-113.

Navaranjan N, Blaikie RJ, Parbhu AN, Richardson JD, Dickson AR (2008) Atomic force microscopy for the measurement of flexibility of single softwood pulp fibres. J Mater Sci 43(12):4323-4329.

Ochi S (2010) Tensile properties of kenaf fiber bundle. SRX Materials Science, Vol. 2010, Article ID 152526, 6 pp. (doi:10.3814/2010/152526, Accessed July 25, 2011).

Page DH, El-Hosseiny F (1983) The mechanical properties of single wood pulp fibres: Part VI. Fibril angle and the shape of the stress–strain curve. J Pulp Paper Sci 9(1-2):99-100.

Rao KMM, Rao KM (2007) Extraction and tensile properties of natural fibers: Vakka, date and bamboo. Compos Struct 77(3):288-295.

Symington MC, Banks WM, West OD, Pethrick RA (2009) Tensile testing of cellulose based natural fibers for structural composite applications. J Composite Mater 43(9):1083-1108.

Tan EPS, Lim CT (2004) Novel approach to tensile testing of micro- and nanoscale fibers. Rev Sci Instrum 75(8): 2581-2585.

Tan EPS, Lim CT (2006) Mechanical characterization of nanofibers—A review. Compos Sci Technol 66(9): 1102-1111.

Tchepel M, Provan JW, Nishida A, Biggs C (2006) A procedure for measuring the flexibility of single wood-pulp fibres. Mechanics of Composite Materials 42(1):83-92.

Xing C, Wang SQ, Pharr GM (2009) Nanoindentation of juvenile and mature loblolly pine (*Pinus taeda* L.) wood fibers as affected by thermomechanical refining pressure. Wood Sci Technol 43(7-8):615-625.

Xue Y, Du Y, Elder S, Wang K, Zhang J (2009) Temperature and loading rate effects on tensile properties of kenaf bast fiber bundles and composites. Compos, Part B Eng 40B(3):189-196.